

Effects of Roughness on Scatterometry Signatures

M. Foldyna¹, T. A. Germer², and B. C. Bergner³

¹Laboratory of Interfaces and Thin Films, CNRS, Ecole Polytechnique, 91128 Palaiseau, France

²National Institute of Standards and Technology, 100 Bureau Drive, Gaithersburg, MD 20899, USA

³Spectrum Scientific, Inc., 16692 Hale Avenue, Irvine, CA 92606, USA

Abstract. We used azimuthally-resolved spectroscopic Mueller matrix ellipsometry to study a periodic silicon line structure with and without artificially-generated line edge roughness (LER). Grating profiles were determined from multiple azimuthal configurations, focusing the incident beam into a 60 μm spot. We used rigorous numerical modeling, taking into account the finite numerical aperture and determining the profile shape using a four trapezoid model for the line profile. Data obtained from the perturbed and unperturbed gratings were fit using the same model, and the resulting root-mean-square error (RMSE) values were compared. The comparison shows an increase in RMSE values for the perturbed grating that can be attributed to the effects of LER.

Keywords: Diffraction grating, Ellipsometry, Line edge roughness, Mueller matrix, Multi-azimuth method

PACS: 42.79.Dj; 07.60.Fs; 42.62.Eh

INTRODUCTION

Recent developments in optical characterization of periodic structures have expanded the range of experimental methods in order to increase sensitivity to structure parameters and imperfections [1]. A new trend is to examine the potential of Mueller matrix and multi-configuration methods in order to address the most challenging problems in optical metrology. In this work we will present results acquired from periodic line gratings with significant artificially generated line edge roughness (LER). The method used in this work is based on Mueller matrix spectroscopic ellipsometry, which is not limited to just the spectrally resolved reflectance phase and amplitude differences, but provides the phases and amplitudes of the cross polarized reflectances, as well as depolarization.

The multi-azimuth method has been shown to improve the robustness of the analysis of perturbed and unperturbed gratings [2] and to provide an estimate of the model parameter accuracy. Introducing the multi-azimuth method essentially necessitates performing Mueller matrix analysis, because the block off-diagonal elements are no longer zero. Furthermore, measuring Mueller matrices accesses the extra degrees of freedom available to reflection. Lastly, the tight focusing associated with micro-spot ellipsometers creates a range of incident directions, which in turn causes some depolarization. The effect is

most pronounced in spectral regions, where the signal changes very fast [3].

Recent theoretical work focused on the sensitivity of angle-resolved data to LER [4,5], demonstrating the significance of the problem and exploring the limits of effective medium approximations. In this work, we are focused on modeling periodically-perturbed structures (see Fig. 1) using the rigorous coupled-wave method and evaluating the sensitivity of experimental spectrally-resolved data to the dimensional parameters of LER.

EXPERIMENTAL DETAILS

Samples description

The sample gratings were manufactured using electron beam lithography followed by etching to make 300 nm grating lines into a silicon wafer. The nominal height and the pitch of the grating are 400 nm and 736 nm, respectively. A scanning electron microscopy (SEM) image of the unperturbed reference grating lines is shown in Fig. 1. The size of the natural line edge roughness (LER) in Fig. 1 is rather small, compared to the line width.

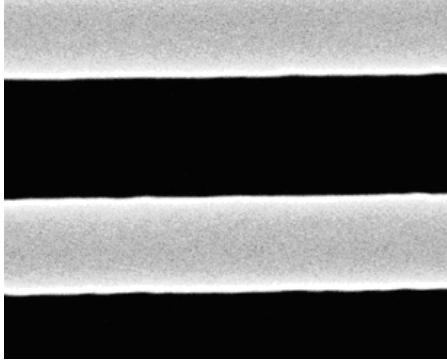


FIGURE 1. Scanning electron microscopy image of the unperturbed reference line grating.

In order to study effects of the LER on the scatterometric data signature, samples with artificially designed roughness were manufactured. The periodic LER designed for the purpose of comparing measured data with a rigorous 2D optical model is shown in Fig. 2. The amplitude of the LER is rather large when compared to the line width, but this was intentional in order to confirm that differences in the data are solely due to LER.

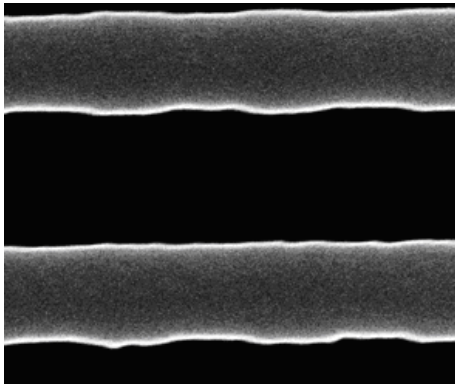


FIGURE 2. Scanning electron microscopy image of the periodically perturbed grating.

Another sample that was manufactured was a line grating with artificially-generated, random, non-periodic LER, shown in Fig. 3. The reference grating for this sample is also part of the same wafer, but its image is not shown here. The sample with non-periodic LER completes the set of samples manufactured for our study of the effects of LER on scatterometric signatures.

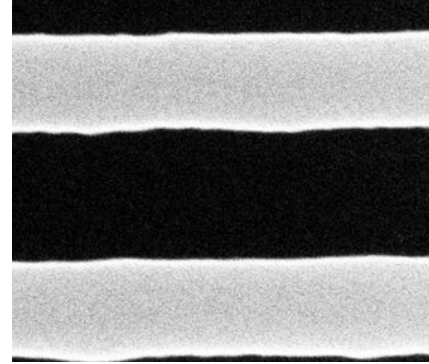


FIGURE 3. Scanning electron microscopy image of the grating with artificially-designed non-periodic LER.

Measurement method

In this work, we used multi-azimuth Mueller matrix ellipsometry to assess the impact of LER on scatterometry data. All measurements were performed using a generalized spectroscopic ellipsometer (M2000F, Woollam¹), which measures eleven elements of the spectrally-resolved, normalized Mueller matrix. The ellipsometer is equipped with fully automated rotational and translational stages and focusing lenses, allowing for measurements with a 60 μm spot size, at a fixed 65° angle of incidence, on multiple targets, and with the incident plane aligned along any azimuth.

Reference and perturbed grating samples are situated in 100 μm \times 100 μm square targets. We have measured targets at multiple azimuthal angles from -90° to 90° while rotating the sample by 5° steps. The data of opposite azimuthal angles were combined together in order to compensate for the missing Mueller matrix elements and to reduce possible influence of systematic experimental errors. The measured data exhibited significant depolarization at some wavelengths, which was caused by the significant numerical aperture (NA) of the focusing optics.

The data measured for each perturbed target were compared with the data for the corresponding reference target. Each set was fit to a 1D model for the grating. Moreover, data for the target with periodic LER was compared to a 2D model for the grating in order to confirm that the observed differences are due to the designed LER.

¹Certain commercial equipment, instruments, or materials are identified in this paper in order to specify the experimental procedure adequately. Such identification is not intended to imply recommendation or endorsement by the National Institute of Standards and Technology, nor is it intended to imply that the materials or equipment identified are necessarily the best available for the purpose.

RESULTS AND DISCUSSIONS

Measurement results

Figure 4 shows the measured data acquired for the azimuthal angle of 45° . Eleven normalized Mueller matrix elements are shown for the case of the reference grating (see Fig. 1), periodically perturbed grating (see Fig. 2), and non-periodically perturbed grating (see Fig. 3). Differences between the data for the reference and periodically-perturbed gratings (black and blue lines in Fig. 4) are very subtle. The data for the non-periodic LER differs from the other two due to the location of that target on a different wafer leading to slightly different line dimensions. Depolarization effects due to finite NA are present in

the data, but they cannot be rigorously estimated as four Mueller matrix elements are not measured. Nevertheless, it is possible to estimate depolarization effects by extending the measured data to complete the Mueller matrices, by assuming perfect symmetry of the gratings.

In special configurations without cross-polarization effects, the depolarization effects can be observed directly in the element M_{22} . Figure 5 shows M_{22} measured for an azimuthal angle of 90° for the non-periodic LER grating and the corresponding reference target. The value of the M_{22} element should be equal to one in this configuration, but the depolarization effects due to the high NA have caused significant dips. The depolarization is not dominated by the presence of roughness, though, since the behavior is similar for both the perturbed and unperturbed gratings.

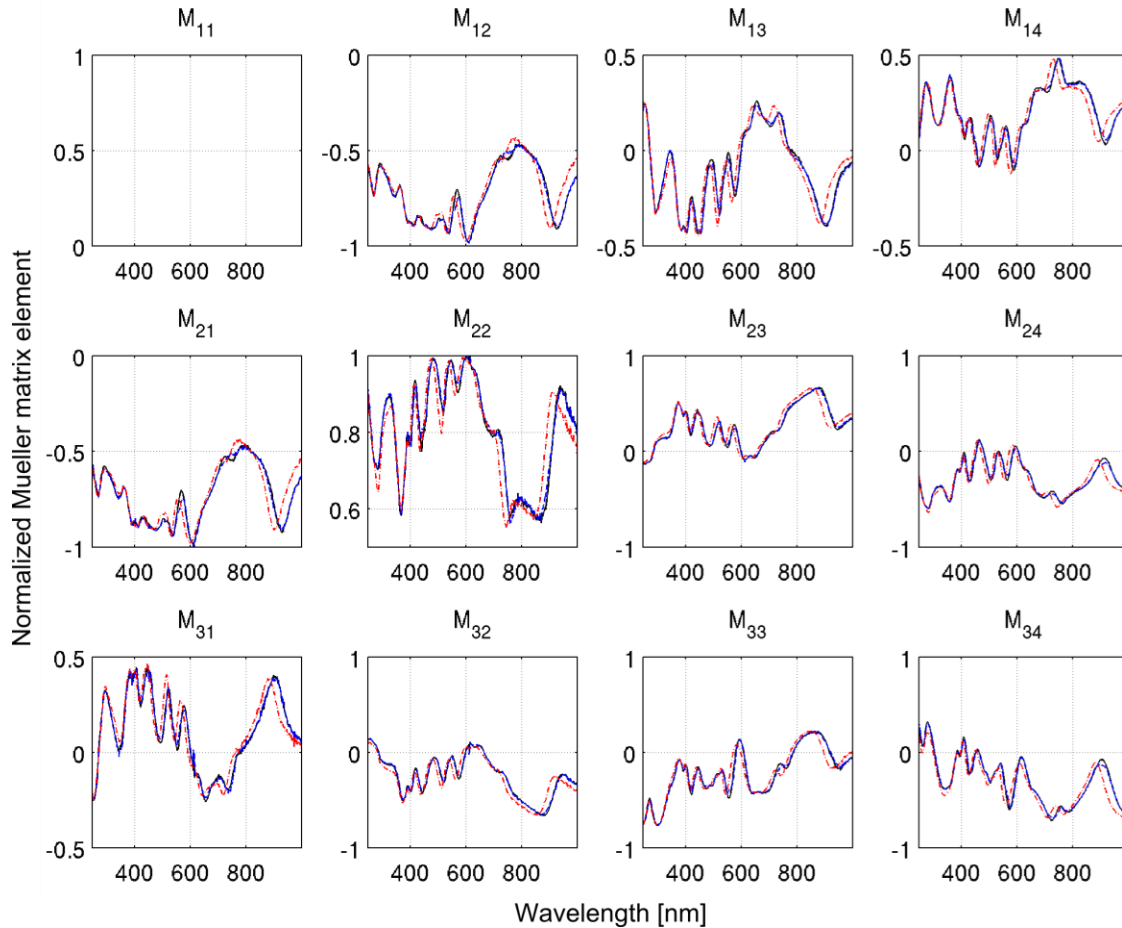


FIGURE 4. Spectrally resolved Mueller matrix elements measured in the reference target (black solid lines), on the periodically perturbed lines (blue dashed lines), and in non-periodic LER target (dash-dotted red lines). The sample was rotated by 45° from the planar geometry.

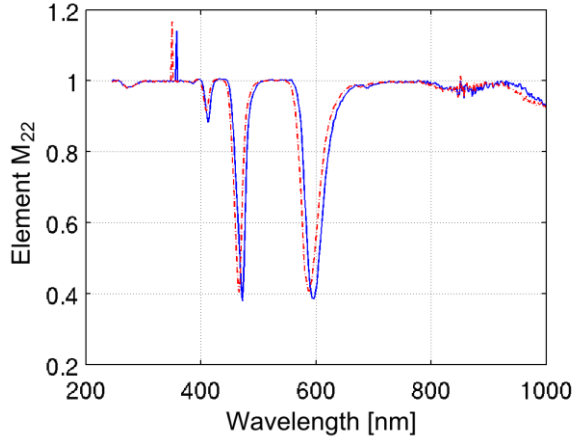


FIGURE 5. Spectral dependence (wavelength is in nanometers) of M_{22} elements measured for 90° azimuth for the reference grating (blue solid lines) and the non-periodic LER grating (red dash dotted lines).

Parametric model of grating profile

Optical response of periodic gratings was modeled using the standard version of rigorous coupled-wave analysis (RCWA) [6,7] extended by implementation of inverse rules [8,9] and the scattering matrix algorithm [10]. The model provides complex elements of 2×2 Jones matrices, which can be easily transformed into 4×4 Mueller matrices. Integration of the Mueller matrix is performed to account for the finite NA.

Calculated Mueller matrices are compared with the measured ones in every step of the optimization procedure searching for the grating profile which best corresponds to the measured data. The merit function is the mean-square error (MSE)

$$\text{MSE} = \frac{1}{N} \sum_{k=1}^{N_s} \sum_{ij \in E} [M_{ij,k}^m - M_{ij,k}^c]^2. \quad (1)$$

Here $M_{ij,k}$ denote the element M_{ij} of the k -th spectral Mueller matrix, which is marked by m for the measured data and c for the calculated data, respectively; N_s and n denote the total number of spectral points and the number of free model parameters, respectively; E is the set of indices for the eleven measured Mueller matrix elements; and the number of degrees of freedom is $N = 11N_s - n - 1$.

Prior to optimization, the profile of the grating must be parameterized and free model parameters defined. The inverse problem of finding optimal values of model parameters has, in principle, a non-unique solution, which puts high demands on a good choice of model parameters and the preselected profile shape. We have carefully selected a model which is reasonably close to typical line profiles and which

introduces only limited correlations between free parameters. Our profile model was composed of four trapezoids and is shown in Fig. 6. Existence of an overhang was confirmed using critical dimension atomic force microscopy [2]. Correlations were high only between some parameters and only for azimuthal angles of 0° and 90° .

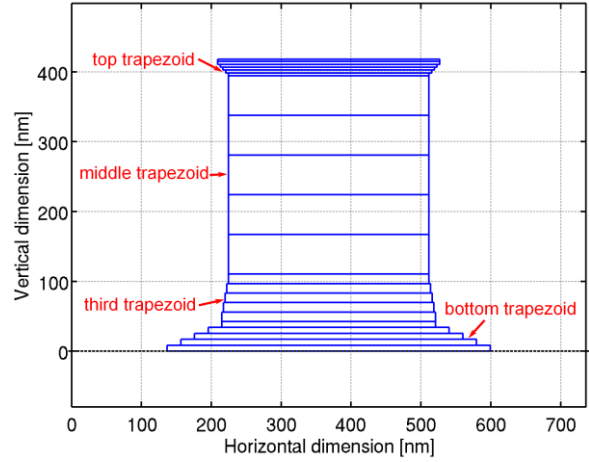


FIGURE 6. Grating profile represented by layers as used directly in the RCWA code. The profile is composed of four trapezoids on top of each other with the clear presence of an overhang on the top of the grating.

We have used eleven model parameters as follows: the total height of the lines; the heights of the top, third, and bottom trapezoids; four trapezoid base widths and the top width; an offset to the nominal azimuthal angle; and the thickness of a silicon dioxide layer on the top of the lines. The best profile was determined for every azimuthal angle separately in order to provide statistical information about the confidence intervals of the free parameters. Variation between the best fit middle line widths found for different azimuthal angles was less than 1 nm.

Detection of line edge roughness

In order to compare quality of all fits, the root-mean-square error (RMSE) defined as $\text{RMSE} = (\text{MSE})^{1/2}$ has been used. Figure 7 shows the azimuthal dependence of best fit RMSE values acquired for the periodically perturbed line grating and its corresponding reference target. RMSE values for the reference target (blue squares) are smaller than for the periodically perturbed grating (red circles), showing that if the one-dimensional RCWA model is used, the designed roughness leads to a significantly poorer fit. This conclusion has been confirmed by applying a rigorous two-dimensional model, which resulted in a decrease of RMSE values for the perturbed grating to

the same level as that observed for the reference target [2]. The increase of RMSE values is observed consistently for all azimuthal angles, confirming high sensitivity of our method to line edge perturbations and allowing us to exclude the dependence of the results on the selected profile model.

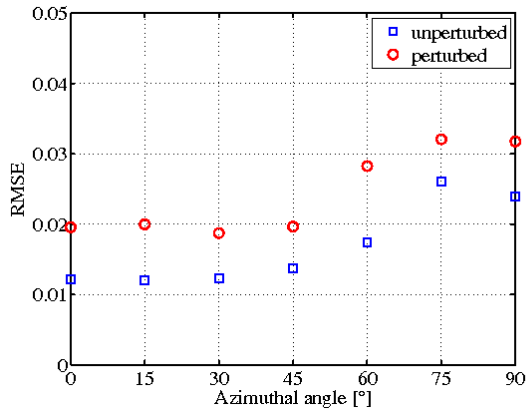


FIGURE 7. Azimuthal dependence of RMSE from the best fits of the reference grating using the one-dimensional RCWA model (blue boxes) and the perturbed grating using the one-dimensional RCWA model (red circles).

In order to investigate the effects of more natural LER, we have done the same study for the line grating shown in Fig. 3. Figure 8 shows the RMSE values plotted for the randomly perturbed grating and its corresponding reference grating. The trend of the azimuthal dependence is the same as in the previous case (Fig. 7), although there are some important differences. RMSE values for the reference target are slightly larger than in the previous case, especially for smaller azimuthal angles. That means that even reference gratings are not identical from wafer to wafer. Also, the contrast between the RMSE values is much smaller than in the previous case. This has been caused by root-mean-square roughness being smaller for the randomly rough target and the roughness being considerably smoother (compare Figs. 2 and 3). Results show that we are still sensitive to the presented LER, although we are close to the limits of the sensitivity in the randomly rough case. Sensitivity may be further improved by using a more accurate profile model, which would yield a better RMSE value for the reference grating.

CONCLUSIONS

We have demonstrated some advantages of our multi-azimuth Mueller matrix ellipsometry method and its sensitivity to perturbation, periodic or random, of the grating lines. Advantages included the ability to measure and model depolarizing effects and an

increased robustness due to the use of the multi-azimuth approach.

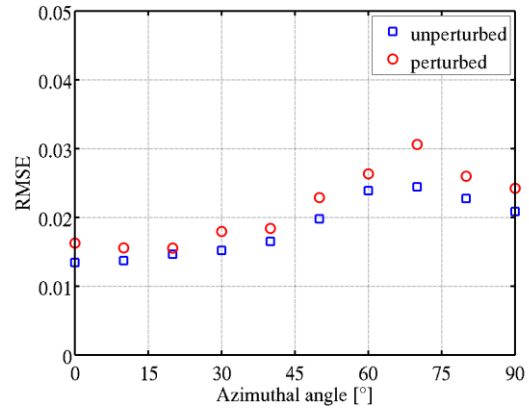


FIGURE 8. Azimuthal dependence of RMSE acquired by fitting reference (blue boxes) and non-periodic LER line gratings (red circles).

REFERENCES

1. R. Silver, T. Germer, R. Attota, B.M. Barnes, B. Bunday, J. Allgair, E. Marx, and J. Jun, Proc. SPIE **6518**, 65180U (2007).
2. M. Foldyna, T.A. Germer, B.C. Bergner, and R.G. Dixon, Thin Solid Films **519**, 2633–2636 (2011).
3. T.A. Germer and H.J. Patrick, Proc. SPIE **7638**, 76381F (2010).
4. B.C. Bergner, T.A. Germer, and T.J. Suleski, Proc. SPIE **7272**, 72720U (2009).
5. B.C. Bergner, T.A. Germer, and T.J. Suleski, J. Opt. Soc. Am. A **27**, 1083–1090 (2010).
6. M.G. Moharam and T.K. Gaylord, J. Opt. Soc. Am. A **7**, 811–818 (1981).
7. M.G. Moharam and T.K. Gaylord, J. Opt. Soc. Am. A **73**, 1105–1112 (1983).
8. P. Lalanne and G.M. Morris, J. Opt. Soc. Am. A **13**, 779–784 (1996).
9. L. Li, J. Opt. Soc. Am. A **13**, 1870–1876 (1996).
10. L. Li, J. Opt. Soc. Am. A **13**, 1024–1035 (1996).